Advances in Science and Technology Research Journal

Advances in Science and Technology Research Journal 2023, 17(3), 64–72
https://doi.org/10.12913/22998624/163108
ISSN 2299-8624, License CC-BY 4.0

Received: 2023.03.20
Accepted: 2023.05.10
Published: 2023.06.01

New Methodology for Predicting the Cracking Phenomenon in the Radial Extrusion Process of Hollow Parts with a Flange

Grzegorz Winiarski[1*], Grzegorz Samołyk[1]

[1] Lublin University of Technology, 38D Nadbystrzycka Str., 20-618 Lublin, Poland
* Corresponding author's e-mail: g.winiarski@pollub.pl

ABSTRACT
The selected issue of flange cracking in the radial extrusion process of hollow parts has been discussed in this paper. The researches were carried out based on numerical calculations in the Deform 3D software and experimental tests, which were carried out using pipe billets made of aluminum alloy EN AW 6063. A new methodology has been developed that allows to determine the place and approximate moment of material cohesion loss. This is determined from the results of the FEM calculation only, and does not require calibration tests. The method is based on a detailed analysis of the state of stress, state of strain in the extruded part, and is focused on identifying zones with an uneven distribution of the mentioned parameters. Determination of characteristic zones with a zero increase in the strain effective value makes it possible to determine, with a high approximation, the maximum (due to the phenomenon of cracking) diameter of the flange. The results of numerical calculations showed a high agreement with the results of experimental tests, in which the maximum diameter of the flange was determined.

Keywords: cracking, extrusion, hollowed parts, flanging, cold forming.

INTRODUCTION

Radial extrusion is an one among many of methods that enable the forming of hollow parts with flanges or lateral protrusions [1]. In many cases, the process is carried out using a mandrel or an additional medium that supports the shaping of the product's hole [2, 3]. In this way, parts with constant or variable wall thicknesses can be obtained from a tubular billet [4]. The maximum dimensions of extruded flanges are limited by the occurrence of undesirable phenomena accompanying forming. These can include: local buckling of the billet wall, foldings, variable thickness of the flange, cracks in the material [5]. The geometry and dimensions of the tools and billet, the thermal parameters of the process and the type of billet material are the key process parameters which are affecting the aforementioned phenomena [6]. Selection of the correct process parameters is facilitated by numerical modeling using the finite element method (FEM). Among the above-mentioned limitations, material fracture prediction poses significant problems in the FEM calculations. During radial extrusion process, the material's fracture occurs when the diameter of the flange exceeds a certain limit, while crack initiation takes place at the flange's lateral surface [7]. Determination of the moment of crack initiation by numerical methods, as in many other technologies, is possible through the use of appropriate criteria. Non-associated failure criteria are most often used in the FEM calculations. They are described by an integral from a certain function, the value of which depends on the state of stress and strain that occurs in the material. The mentioned criteria include: Cockroft-Latham [8], Freudenthal [9], Brozzo [10], Norris [11], Ayad [12], Rice-Teracey [13], Argon [14], Zhan [15], Oyan [16], Ko [17]. Application of the above relationships requires knowledge of the value of the limiting integral, which is determined experimentally in appropriate calibration tests. Wierzbicki et al [18] performed calibrations for seven fracture criteria

using fifteen tests in which the specimen shape was: round, flat, cylinder, plate, dog-bone, pipe, solid bar. Obtained results show that some criteria are correct only within a limited range of the stress state described by stress triaxiality. Lou et al [19] also used different sample shapes to calibrate the fracture criterion recommended for sheet metal forming processes. Pater et al [20] proposed that the values of limit integrals for rotational forming processes can be determined by the cross-wedge rolling method using conical-cylindrical samples. On the other hand, results described in the papers [21, 22], present a new method in which the values of limit integrals are determined using the rotary compression method. In another study [23], the authors analyzed the Oyane criterion, for which the limit integral was determined using the skew rolling of conical specimens method. For example in a study [24], there is a list of the values of limit integrals for different criteria determined for R200 and 100Cr6 steels in hot tensile testing. For a given material, the value of the limit integral significantly depends on the temperature. The research that has been carried out in the field of fracture prediction indicates that the criteria and tests for their calibration are not always in agreement with experimental results. Watanabe [25] showed that in the cold forging process of a stepped hollow shaft, the Cockcroft Latham criterion does not indicate the correct fracture location. Similar conclusions have been presented in the paper [26] on the example of the process of orbital forging of a flange pin. Therefore, the researchers proposed their own equations that gives better results. Prediction of crack location is made on the basis of analysis of stress components of a polar coordinate system and equivalent stress. Also, Pater et al [27] showed that during cross wedge rolling of harrow tooth preforms, the location of the developing cracks does not agree with those indicated by currently known criteria. The best agreement of the results was obtained using the Cockroft-Latham, Freudenthal and Argon criteria for the zones of the material where the stress triaxiality is greater than 0.33. In the remaining locations where the stress triaxiality is less than 0.33, the tested energetic criteria are ineffective. Therefore, the authors proposed their own fracture criterion [28], which is a combination of the maximum shear stress criterion and the Oh criterion. The influence of each criterion on the value of the new hybrid criterion depends on the stress state described by stress triaxiality.

Based on a review of the literature, it has been found that the cracking phenomenon is a complicated and difficult issue for numerical modeling. The prediction of material cracking bases on various criteria, the correspondence of which with the results of experimental tests is highly different. The accuracy of each criterion depends on the stress state occurring during the forming of the part and on the knowledge of the criterion's limit value, determined by calibration tests. The best results are obtained in the cases where the stress and strain state of the reference specimen during the calibration test is very similar to the stress and strain state of the material during the forming of the part. Therefore, new criteria and new calibration tests which are dedicated to strictly defined technologies still are being developed. Therefore, it was considered reasonable to undertake research in this area. This paper presents a new methodology for determining the location and moment of flange cracking in the radial extrusion process of a hollow part. The proposed method bases on the analysis of the state of stress and strain, therefore its application does not require a calibration test. The purpose of the paper is verification of the adopted assumptions based on theoretical and experimental studies, which were realized for tubular billets made of aluminum alloy EN AW 6063.

RESEARCH METHODOLOGY

The process of radial extrusion was realized according to the scheme shown in Figure 1a. The pressure of the punch 1 on the top surface of the tubular billet 2a causes the filling of the impression formed between the container 3 and the base 4. The height h of the impression was assumed to be equal to the wall thickness g of the billet. The dimensions of the tools and the billet are listed in Table 1. Aluminum alloy EN AW 6063 in the annealed state was used as the extruded material, which was deformed under cold forming conditions to obtain a extruded part with an outer flange 2b with a diameter D. The annealing process was realized in an electric chamber furnace, where the specimens were held at a temperature of 415 °C for 2 hours, after which they were slowly cooled together with the furnace. Numerical calculations were performed by the finite element method using the Deform 3D software. In the process of the billet discretization, the tetragonal four-node

elements were used in the amount of about 200 thousand. The flow curve of the analysed alloy was described by the constitutive equation, which was determined by own tests in the annealed cylindrical specimens upsetting test. Cylindrical specimens were made from the same bar from which the tubular billets were made. Based on the data from the upsetting test for each measurement point, the value of the yield stress as a function of strain was determined from the relation (1) and (2). The experimentally determined flow curve was described by a constitutive Equation 3. To determine the coefficients C, n of the Equation 3, the function described by the Equation 4 was defined. The minimum of the function (4) was determined by using the Generalized Reduced Gradient optimization method implemented in Microsoft Excel. Based on the calculations the flow curve was described by the Equation 5.

$$\varepsilon_i = \ln\frac{h_0}{h_i} \tag{1}$$

$$\sigma_i = \frac{4 \cdot F_i \cdot h_i}{\pi \cdot d_0^2 \cdot h_0} \tag{2}$$

where: ε_i, σ_i – value of strain and yield stress at the i-th experimentally measurement point;
h_0, d_0 – initial height and diameter of the cylindrical specimens;
h_i, F_i – the temporary height of the cylindrical specimen and the corresponding temporary force.

$$\sigma_p = \mathrm{C} \cdot \varepsilon^{\mathrm{n}} \tag{3}$$

where: σ_p – yield stress in MPa;
ε – strain.

$$\Delta = \Sigma_{i=1}^{n}\left[\sigma_i - \sigma_{pi}\right]^2 \rightarrow min \tag{4}$$

where: σ_{pi} – the value of the yield stress determined from the constitutive equation.

$$\sigma_p = 147.5 \cdot \varepsilon^{0.2} \tag{5}$$

The contact conditions between the billet and the tools were described with a shear friction model using a friction factor equal to m = 0.2. A constant punch movement speed equal to 50 mm/min was defined. The initial temperature of the tools and the billet was assumed to be 20 °C, while the heat transfer coefficient between the abovementioned objects was assumed to be equal to 10 kW/m²K. On the outer lateral surface of the billet at a distance from the base equal to half of the height of the impression, 180 sensors were placed uniformly around the circumference in such a way that sensor No. 1 was located between sensor No. 180 and sensor No. 2, sensor No. 2 was

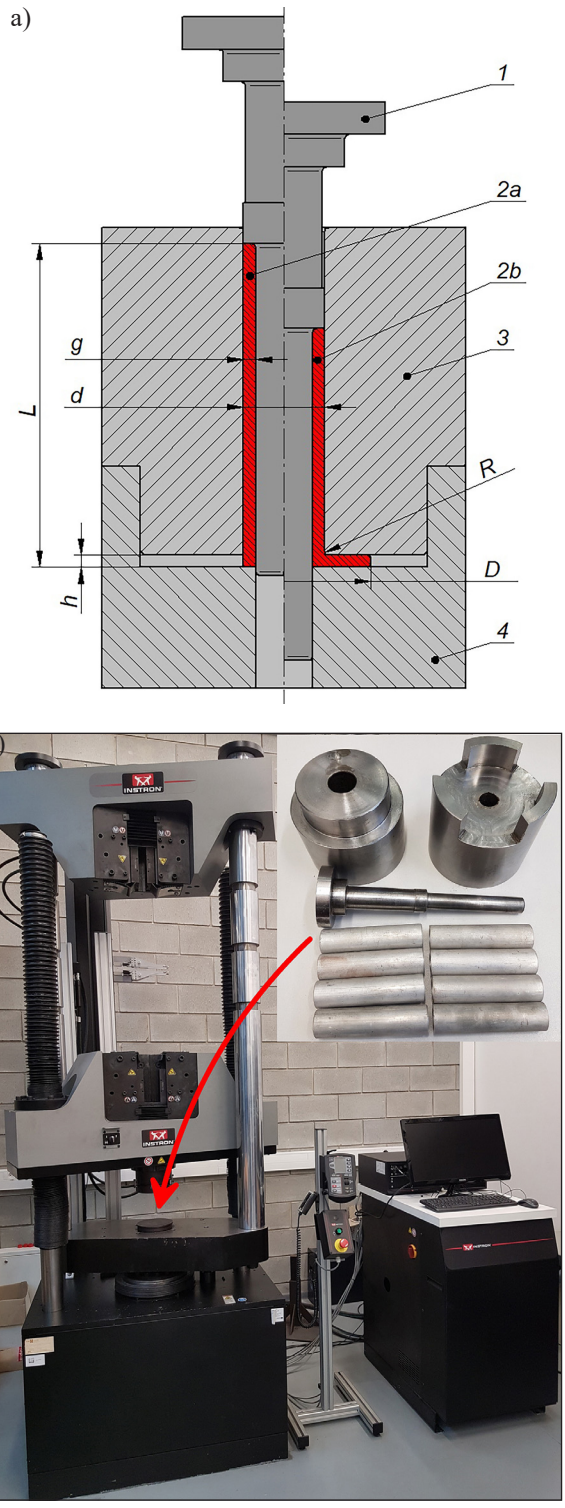

Figure 1. Conditions for the realization of the radial extrusion process: a) process scheme, b) tools, billet and Instron 1000 HDX testing machine

Table 1. Dimensions of tools and billet (designations according to Figure 1)

L, [mm]	*d*, [mm]	*g*, [mm]	*h*, [mm]	*R*, [mm]
80	20	3	3	1

located between sensor No. 1 and sensor No. 3, and so on. The sensors moved together with the deformed material, enabling detailed analysis of the state of stress and strain on the lateral surface of the extruded flange.

Experimental research was carried out using the equipment shown in Figure 1b. The tools were placed in the work space of an Instron 1000 HDX testing machine. Before the extrusion process, the tubular billets were lubricated by oil with molybdenum disulfide. A force applied to the punch was measured as a function of its displacement. The extrusion process was carried out until the flange cracked, which made it possible to determine its maximum diameter.

Based on experimental results and analysis of numerical calculations, a new methodology has been developed for predicting the moment and location of flange cracking. In practice, this new method bases only on FEM results.

DISCUSSION

On the basis of the experimental results, the numerical model of the radial extrusion process was validated, additionally, the diameter of the flange at which cracking occurs was determined, too. Figure 2a shows axial cross-sections of the obtained extruded part. The geometry of those parts obtained in the experimental tests is the same as that obtained in the FEM calculations. In both cases, the flange has a variable thickness, which decreases as its diameter increases. Qualitative and quantitative agreement of the results was also obtained in terms of the inclination of the flange edge from the surface of the extruded part base (perpendicular to the axis of symmetry of the extruded part). The force parameters of the process were also examined. The courses of forces applied to the punch as a function of its displacement are shown in Figure 2b. Both in the experimental tests and in the FEM calculations, the value of the force increases with the progression of the process. This is caused by an increasing diameter of the flange. In quantitative aspect, it can be said that the values of the force required for the experimental tests at the initial stage of the process are smaller than those determined by FEM calculations. On the other hand, in the further stage of this process, the force determined theoretically reaches smaller values than in real conditions. This is caused by variable lubrication conditions. In the FEM calculations, a constant value of the friction factor was assumed, while in real conditions, the lubrication efficiency of the contact surfaces of the billet with the tools decreases due to the relative motion of the aforementioned objects, which causes the breaking of the lubrication film. Therefore, the force parameters determined in the simulation in terms of quality and quantity should be considered as compatible with the experimental results. In conclusion, it can be said that, the numerical model of the process has been built correctly and represents the analyzed real extrusion process.

Based on experimental tests, the diameter of the flange at which the crack appears was determined. It was considered the maximum value due to the phenomenon of material crack. The diameter value determined in this way is D = 44mm. The crack appears on the lateral surface of the flange (Figure 2c). Around the crack, a local thinning of the material is visible, resulting from the concentration of strain around the crack center.

The estimation of the possibility of material cohesion loss was made out based on the results of numerical calculations. This estimation was begun with analyzis one of the fracture criteria. The normalized Cockcroft Latham fracture criterion described by Equation 6 was selected, in which the possibility of material cracking is predicted on the basis of knowledge of the highest principal stress and stress intensity for a specific point.

$$\int_0^{\varphi_{gr}} \frac{\sigma_1}{\sigma_i} d\varphi = C \tag{6}$$

where: σ_1 – maximum principal stress;
σ_i – effective stress;
φ – effective strain;
C – material's constant value.

The distribution of the values of the aforementioned integral for the extruded part is shown in Figure 3, which also shows the courses of change in the values of this integral for all 180 sensors. Due to the large number of curves (as in the following figures), no legend is given. These curves create a characteristic pattern defining a range of

values of the studied quantity, which at the same time illustrates its characteristics, depending on the range of values. Several zones are visible at the flange edge where the integral values are larger than in their direct surroundings. In addition, a continuous increase in the integral value is observed in these zones while in their surroundings the integral values have stayed constant since a certain moment. The constant value of the function (6) in the running process means that the value of the quotient of the maximum principal stress and the effective stress from a certain moment reaches a value equal to 0 or there is no increase in strain in the discussed areas. Therefore, the value of the aforementioned quotient for all sensors during the extrusion process is shown in Figure 4. It can be seen that the curve pattern is concentrated in a close range of values, creating a visible trend. In the steady-state phase of flange forming (from about the 5th second of the process time), the value of the quotient is almost constant at about 1. This means that the maximum principal stress is equal to the effective stress. Therefore, there is no stress disappearance in any sensor, so the value of the Cockroft Latham integral should not be equal to 0. Therefore, Figure 5 shows the distribution of strain on which it is possible to identify zones in which the value of strain does not increase since a certain moment. This explains the constant value of the integral in these areas. In addition, between the above-defined areas, a continuous increase in the strain value can be observed. This means that on the circumference of the flange, there are zones where the strain is concentrated, and which are surrounded by dead zones where the strain increase is smaller or zero. The values of strain increase described by relation (7) for individual sensors are shown in Figure 6.

$$\Delta\varphi_i = \frac{\varphi_{i+1} - \varphi_i}{\varphi_i} \cdot 100\% \qquad (7)$$

where: $\Delta\varphi_i$ and φ_i – the increase in strain and the strain value, respectively, in the i-th calculation step of the analyzed process.

Until about the 5th second of the process, the increase in strain measured for each sensor is relatively high and rapid. This is the initial phase of the process, in which the tube material begins to fill the impression formed between the container and the base. In the further stage of extrusion, there is a stable increase in the diameter of the flange, in which the strain increase is smaller and has a more stable course. There are some sensors for which, since about 23 s of the process, the increase in strain is zero (the blue vertical dashed line on the graph), while in the other sensors the strain value increases continuously. The distribution of strain increase for individual sensors at selected time steps is shown in Figure 7. There are two zones around the circumference of the flange (sensors 105–110 and 125–130), where the strain increase is zero from 23.3 seconds of the process.

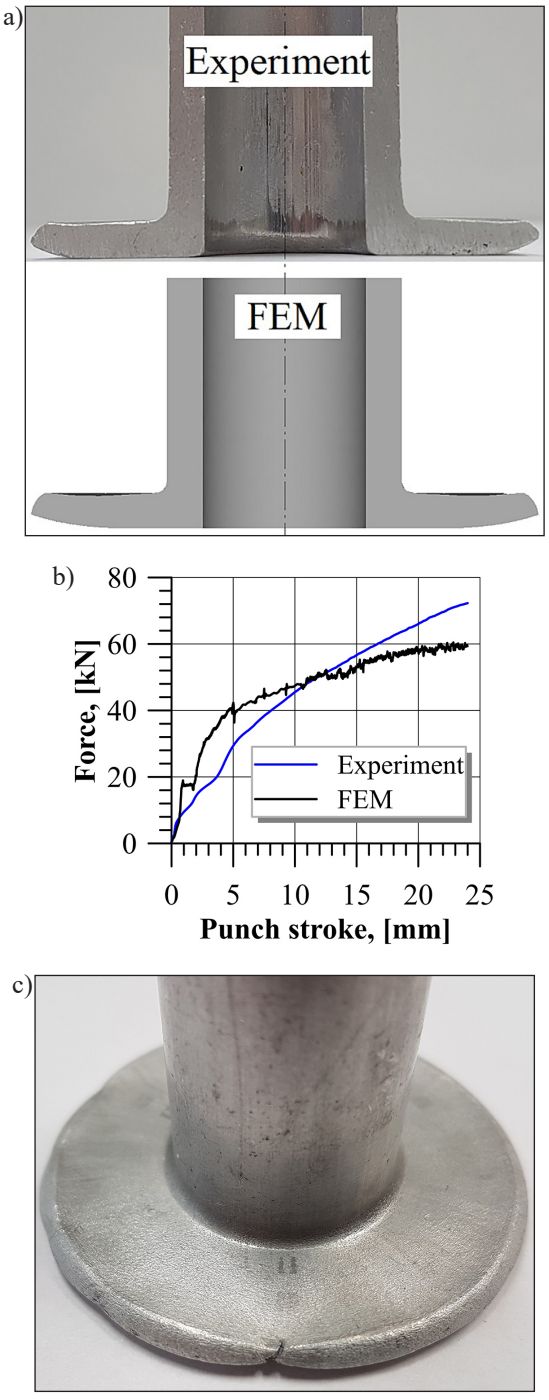

Figure 2. Experimental and FEM results: (a) extruded parts in axial cross-section, (b) force, (c) flange with crack

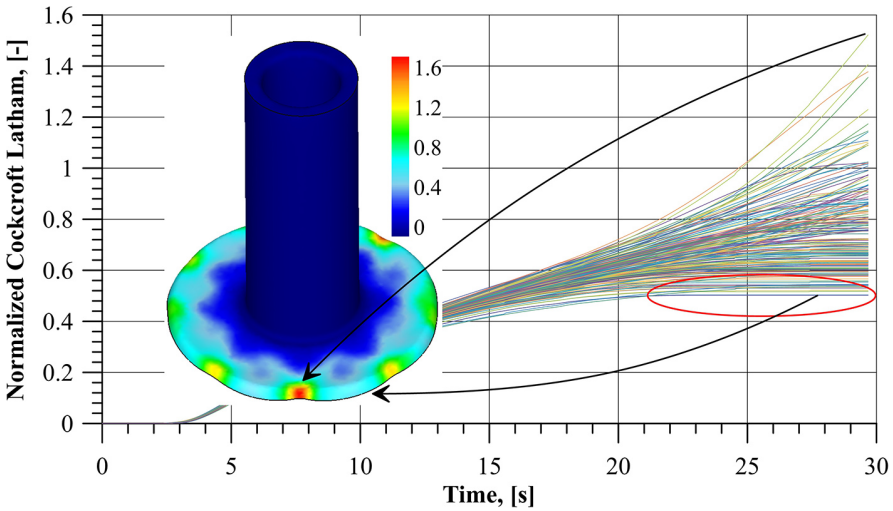

Figure 3. Distribution of integral values according to the normalized Cockcroft Latham cracking criterion (description in the text)

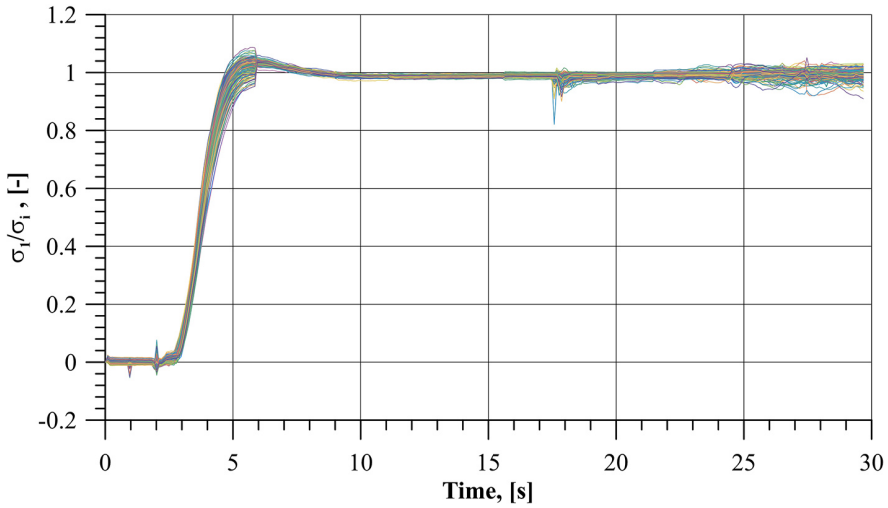

Figure 4. The value of the quotient of the maximum principal stress and effective stress for individual sensors (description in the text)

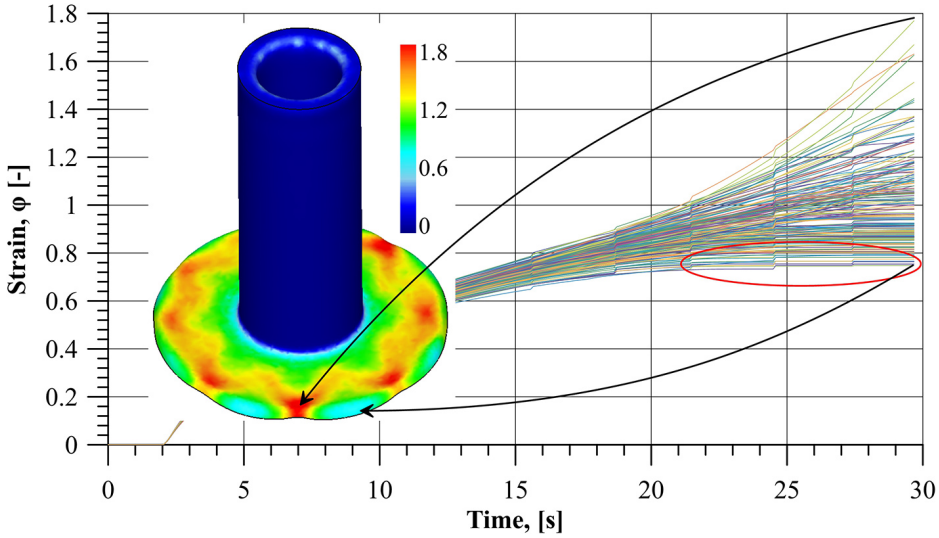

Figure 5. Distribution of effective strain values (description in the text)

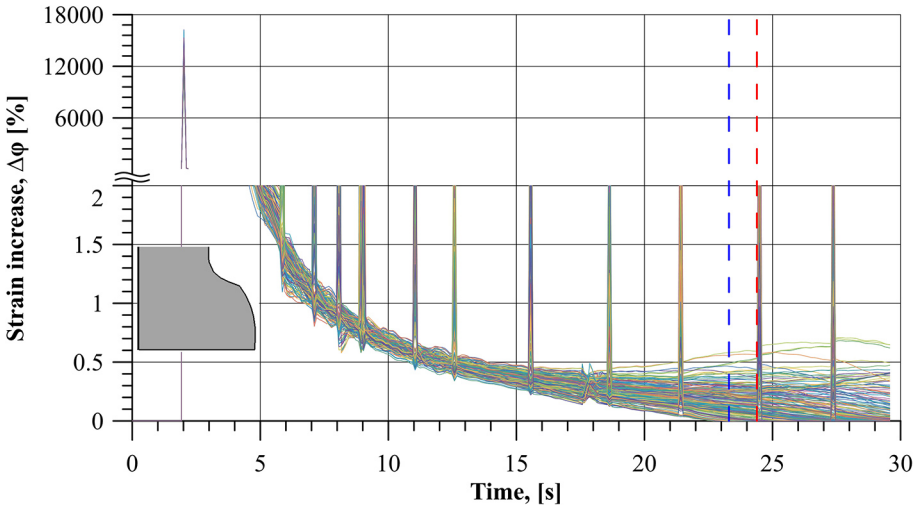

Figure 6. Increase in effective strain values for individual sensors (description in the text)

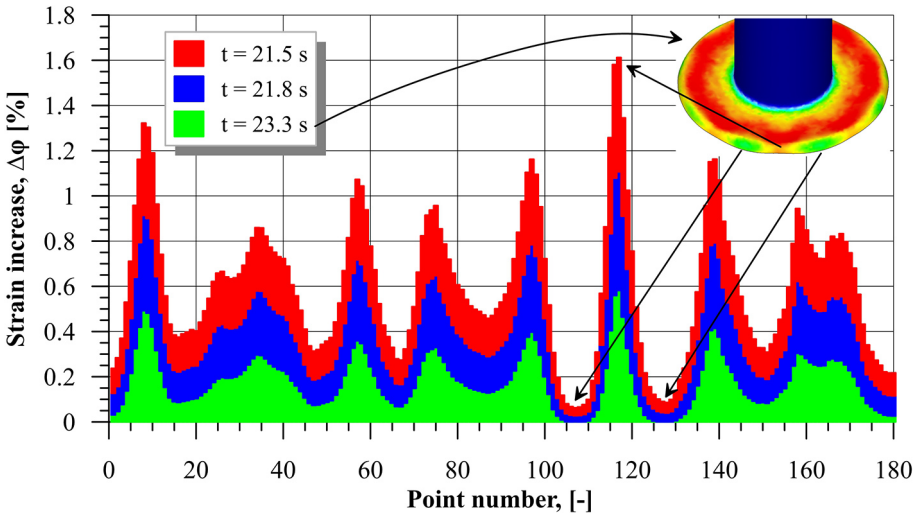

Figure 7. Increase in effective strain values for individual sensors at selected extrusion stages

In addition, between these zones there is an area (sensors 115–120) where the strain increase is the highest. This is an area of strain concentration, which is surrounded by two dead zones, which indicates the location of the material fracture. The moment of flange cracking (flange achieves a diameter equal to D = 44mm, it is shown by the red vertical dashed line in Figure 6), determined experimentally, occurs about 1 second after the appearance of zones of zero strain increase (then the flange has a diameter equal to D = 43.3mm). Therefore appearance of two zones with zero increase in strain between which there is an area of highest value of strain means that further realization of the extrusion process will cause cracking of the flange in a relatively short time. The study shows that a detailed analysis of the state of strain makes it possible to determine the moment and location of cracking of a flange formed by radial extrusion from a tubular billet with a very good approximation.

CONCLUSIONS

The theoretical and experimental studies has been performed on the process of radial extrusion of flanges in hollow products. The obtained results of these studies lead to the following conclusions:

1. Detailed analysis of the FEM results makes it possible to determine the location and approximate moment of flange cracking in radial extrusion process,
2. The distribution of integral values according to the normalized Cockcroft Latham fracture criterion and the distribution of effective strain

in the flange is not uniform; at the edge of the flange, zones of local concentration of the mentioned parameters are formed, which are surrounded by areas where the values of the these parameters are smaller,

3. At a certain moment of extrusion, two dead zones appear, in which the strain value remains constant; between these zones, appear a region in which the strain values are highest around the circumference of the flange; the appearance of these zones indicates the location and approximate moment of cracking of the material,
4. A further direction for the development of the presented method can be research in the field of fracture analysis of extruded parts made of different materials.

Acknowledgments

The research was financed from the funds of the Scientific Discipline Council for Mechanical Engineering: M/KOPM/FD-20/IM-5/132/2022.

REFERENCES

1. Ma Y., Qin Y., Balendra R. Upper-bound analysis of the pressure-assisted injection forging of thick-walled tubular components with hollow flanges. International Journal of Mechanical Sciences 2006; 48: 1172–1185.
2. Ma Y., Qin Y., Balendra R. Forming of hollow gear-shafts with pressure-assisted injection forging (PAIF). Journal of Materials Processing Technology 2005; 167: 294–301.
3. Qin Y., Ma Y., Balendra R. Pressurising materials and process design considerations of the pressure-assisted injection forging of thick-walled tubular components. Journal of Materials Processing Technology 2004; 150: 30–39.
4. Szala M., Winiarski G., Bulzak T., Wójcik Ł. Microstructure and hardness of cold forged 42CrMo4 steel hollow component with the outer flange. Advances in Science and Technology Research Journal 2022; 16(4): 201–210.
5. Lin S.Y., Lin F.C. Predictions of the minimum relative depth of die cavity and the minimum amount of preforming in the radial extrusion of tubular components. Computers & Structures 2006; 84(7): 503–513.
6. Winiarski G., Gontarz A., Samołyk G. Theoretical and experimental analysis of a new process for forming flanges on hollow parts. Materials 2020; 13(4088).
7. Gronostajski Z., Pater Z., Madej L., Gontarz A., Lisiecki L., Lukaszek-Solek A., Luksza J., Mróz S., Muskalski Z., Muzykiewicz W., Pietrzyk M., Sliwa R.E., Tomczak J., Wiewiórowska S., Winiarski G., Zasadzinski J., Ziólkiewicz S. Recent development trends in metal forming. Archives of Civil and Mechanical Engineering 2019; 19: 898–941.
8. Zhan M., Ch. Gu, Zhiqiang J., Lijin H., He Y. Application of ductile fracture criteria in spin-forming and tube-bending processes. Computational Materials Science 2009; 47: 353–365.
9. Xunzhong G., Fuye M., Qun G., Xinyi L., Naksoo K., Kai J. A calculating method of tube constants of ductile fracture criteria in tube free bulging process based on M-K theory. International Journal of Mechanical Sciences 2017; 128–129: 140–146.
10. Li H., Fu M.W., Lu J., Yang H. Ductile fracture: Experiments and computations. International Journal of Plasticity 2011; 27: 147–180.
11. Walczuk-Gągała P., Pater Z., Wójcik Ł. Determination of the value of the damage function in 1050A aluminium alloy. Advances in Science and Technology Research Journal 2020; 14(2): 49–55.
12. Pater Z., Tomczak J., Bulzak T., Wójcik Ł., Walczuk-Gągała P. Rotational compression of cylindrical specimen as a new calibrating test for damage criteria. Materials 2020; 13(740).
13. Pater Z., Gontarz A., Tomczak J., Bulzak T., Wójcik Ł. Determination of the critical value of material damage in a cross wedge rolling test. Materials 2021; 14(1586).
14. Pater Z., Tomczak J., Bulzak T., Wójcik Ł., Skripalenko M. M. Prediction of ductile fracture in skew rolling processes. International Journal of Machine Tools & Manufacture 2021; 163(103706).
15. Pater Z., Tomczak J., Bulzak T., Knapiński M., Sawicki S., Laber K. Determination of the critical damage for 100Cr6 steel under hot forming conditions. Engineering Failure Analysis 2021; 128(105588).
16. Pater Z., Tomczak J., Bulzak T., Zniszczyński A. The problem of material fracture prediction in cross rolling processes. Advances in Science and Technology Research Journal 2018; 12(4): 184–189.
17. Pater Z., Tomczak J., Bulzak T., Wójcik Ł., Walczuk P. Assessment of ductile fracture criteria with respect to their application in the modeling of cross wedge rolling. Journal of Materials Processing Technology 2020; 278(116501).
18. Wierzbicki T., Bao Y., Lee Y. W., Bai Y. Calibration and evaluation of seven fracture models. International Journal of Mechanical Sciences 2005; 47: 719–743.
19. Lou Y., Huh H. Prediction of ductile fracture for advanced high strength steel with a new criterion:

experiments and simulation. Journal of Materials Processing Technology 2013; 213: 1284–1302.

20. Pater Z., Tomczak J., Bulzak T., Walczuk-Gągała P. Novel damage calibration test based on cross wedge rolling. Journal of Materials Research and Technology 2021; 13: 2016–2025.
21. Pater Z., Tomczak J., Bulzak T., Wójcik Ł., Lis K. Rotary compression in tool cavity- a new ductile fracture calibration test.The International Journal of Advanced Manufacturing Technology 2020; 106: 4437–4449.
22. Pater Z., Tomczak J., Bulzak T. Rotary compression as a new calibration test for prediction of a critical damage value. Journal of Materials Research and Technology 2020; 9(3): 5487–5498.
23. Bulzak T., Pater Z., Tomczak J. Validation of a new system for measuring material constants representing damage limits, Measurement 2022; 196(111265).
24. Pater Z., Gontarz A. Critical damage values of R200 and 100Cr6 steels obtained by hot tensile testing. Materials 2019; 12(1011).
25. Watanabe A., Fujikawa S., Ikeda A., Shiga N. Prediction of ductile fracture in cold forging. Procedia Engineering 2014; 81: 425–430.
26. Samołyk G. Studies on stress and strain state in cold orbital forging a AlMgSi alloy flange pin. Archives of Metallurgy and Materials 2013; 58(4): 1183–1189.
27. Pater Z., Tomczak J., Bulzak T., Bartnicki J., Tofil A. Prediction of crack formation for cross wedge rolling of harrow tooth preform. Materials 2019; 12(2287).
28. Pater Z., Tomczak J., Bulzak T. Establishment of a new hybrid fracture criterion for cross wedge rolling. International Journal of Mechanical Sciences 2020; 167(105274).